

Transformation of a Close-Packed Au Nanoparticle/Polymer Monolayer into a Large Area Array of Oriented Au Nanowires via E-beam Promoted Uniaxial Deformation and Room Temperature Sintering

Shisheng Xiong,^{†,‡} Ryan Molecke,[†] Matthew Bosch,[†] P. Randall Schunk,[‡] and C. Jeffrey Brinker^{*,†,‡}

[†]NSF/UNM Center for Micro-Engineered Materials, Department of Chemical and Nuclear Engineering, The University of New Mexico, Albuquerque, New Mexico 87131, United States

[‡]Advanced Materials Lab, Sandia National Laboratories, 1001 University Boulevard SE, Albuquerque, New Mexico 87106, United States

S Supporting Information

ABSTRACT: Transformation of 2D Au nanoparticle (NP) arrays into large scale, ordered, and oriented nanorod/nanowire arrays supported on a transferrable polymer film has been accomplished. E-beam irradiation followed by room temperature aging of a suspended Au NP/polymethylmethacrylate (PMMA) polymer close packed monolayer results in one-dimensional nanoparticle aggregation, reorientation, and sintering into a high density array of oriented Au nanowires with coherent single-crystal-like interfaces. Molecular dynamics simulations of alkane-thiol capped Au NPs, interacting through the Vincent potential and undergoing 2D Poisson compression, account semiquantitatively for the qualitative features of the transformation. This fabrication approach should be extendable to directing 1D aggregation of highly anisotropic nanostructures in arbitrary NP systems.

Two-dimensional (2D) nanoparticle arrays or superlattices are of physical and chemical interest as analogs to their crystalline counterparts assembled from atoms. To date, well developed colloidal chemistry enables fast and facile synthesis of metallic,¹ semiconductor,^{2–4} and magnetic nanoparticles (NPs)⁵ with precise size and shape control. Further entropy driven self-assembly of monosized and binary NPs^{6–9} has resulted in ordered arrays in which collective electronic, magnetic, and optical properties can be tuned through electron charging and quantum confinement of individual NPs mediated by coupling interactions with neighboring NPs. Despite considerable progress on developing structural perfection of NP arrays, their analogy to atomic solids breaks down with respect to electron transport. Because NPs are stabilized with dielectric organic ligands, NP arrays are insulators and behave as an array of isolated Coulomb islands unless sufficient field strengths are applied to achieve electron tunneling.^{6–8} To facilitate electron transport for optoelectronic applications, tremendous effort has been aimed at modifying the insulating organic capping layer by ligand exchange,⁹ thermal annealing to neck adjacent nanoparticles,⁴ or even metal chalcogenide complexation and conversion to semiconductor phases upon gentle heating, generating inorganic nanocrystal solids.¹⁰

An alternative approach to achieve efficient and directed energy or electron transfer is the assembly of one-dimensional nanoscale building blocks, nanorods, or wires. Reported methods include electric-field assisted alignment,^{11,12} interfacial compression with Langmuir–Blodgett troughs,^{13,14} stream alignment with microfluidics,^{15,16} blown-bubble films,^{17,18} “knocking down” motion,¹⁹ and contact printing.^{20–22} Although significant progress has been made,²³ oriented assembly of nanowires over a large area with side-by-side registry and high density remains a significant challenge.

Here we report the formation of a large scale, ordered, and oriented Au nanowire array by transformation and coalescence of an ordered close-packed gold nanoparticle/polymer monolayer via constrained uniaxial deformation and room temperature sintering induced by electron beam irradiation. This approach results in high densities of integrated single-crystal-like nanowires that exhibit directional metallic conductivity on the macroscale.

2D Au NP/polymethylmethacrylate (PMMA) monolayer arrays (e.g., Figure 1A) were prepared by dispersion of 5.5-nm diameter, alkane-thiol stabilized Au NPs dissolved in a solution of toluene plus PMMA on a water surface. Evaporation induced self-assembly confined to a fluid interface results in a large area ordered NP/PMMA monolayer²⁴ that was transferred²⁵ to a trenched structure, resulting in a constrained, freely suspended film with one free edge (see schematic Figure 3A) aligned in the trench. AFM and X-ray reflectivity experiments determined that the NPs reside exclusively at the original polymer/air interface (as opposed to within the 50-nm thick polymer film or at the original polymer/water interface). The suspended films were then subjected to E-beam irradiation employing current densities in the range of 30–200 pA/cm² and an accelerating voltage of 200 kV (see Supporting Information). TEM imaging (Figure 1) showed that E-beam irradiation causes uniaxial contraction in the direction normal to the free edge, accompanied by only a modest expansion in the corresponding normal direction (Figure 1B). After about 1 min, the NP *d*-spacing was reduced by 20% in the unconstrained direction, forming chain-like aggregates (Figure 1B). Sometimes quasi-square planar NP arrangements were formed, depending on the NP orientation of the parent film, as shown in Figure S2 and simulated in Figure S5). Further aging at room temperature without E-beam irradiation resulted in a more uniform and fused

Received: March 22, 2011

Published: June 28, 2011

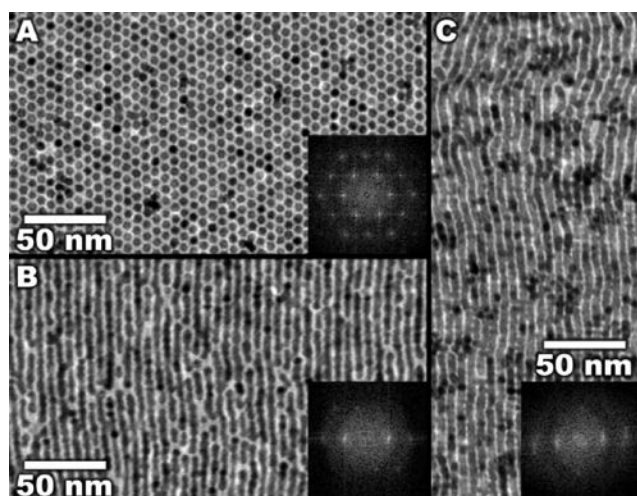


Figure 1. (A) TEM image showing large-area hexagonal close-packed Au NP/PMMA monolayer array prepared by interfacial assembly.²⁴ (B) Typical chain-like nanostructure formed by irradiating the free-standing NP/PMMA monolayer array under E-beam for 1 min. (C) Ordered Au nanowire array formed after further aging at RT without E-beam exposure for 7 days.

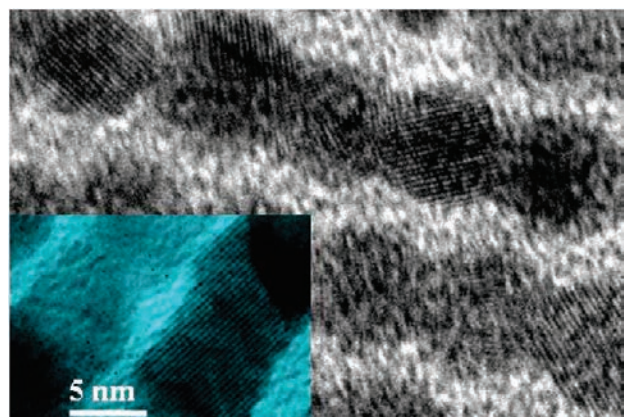


Figure 2. High resolution TEM images demonstrating the initial random configuration of the chain-like aggregates and the single-crystal-like NP interfaces (Inset) that form upon room temperature aging.

nanowire-like array, with wire lengths extending up to several hundred micrometers (Figure 1C).

High resolution TEM imaging showed that the nascent NP aggregates were randomly oriented (Figure 2), but upon aging they coalesced and reoriented into uniform nanowires (Figure 2 inset). In comparison, for completely unconstrained free-standing films, a similar retraction was observed, but the *d*-spacing decreased uniformly in all directions, preserving the original hexagonal arrangement of the NPs. For unsupported oleic acid stabilized PbSe/PMMA monolayer arrays formed as for Au and E-beam irradiated in a similar fashion, linear aggregation occurred but without any observable NP fusion (see supplementary Figure S2).

To explain our experimental results, we propose that E-beam irradiation of PMMA, a positive tone E-beam resist, results in chain scission, reducing its molecular weight and modulus of elasticity. The reduced modulus allows residual stresses that develop upon drying of the transferred film²⁶ and capillary stresses acting on

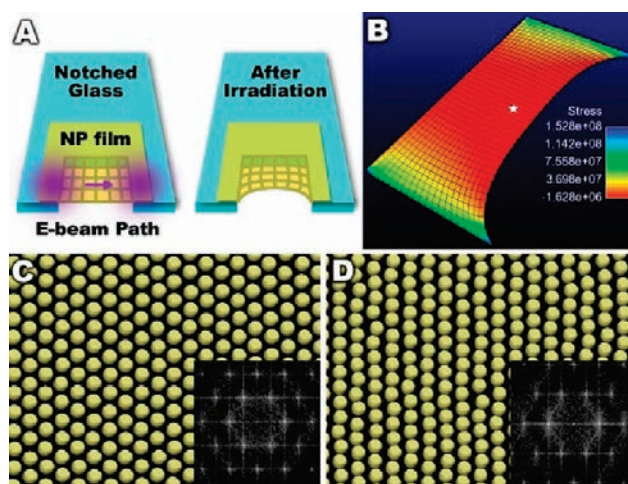


Figure 3. (A) Schematic shows original film configuration and the retraction (upon E-beam irradiation) of the suspended nanoparticle/polymer monolayer array with a free edge. (B) In-plane axial normal stress in receding direction as predicted from a Lagrangian finite element simulation of residual stress relief due to volume change (Dot shows area of MD simulation). (C) Molecular dynamics simulation of original self-assembled NP/polymer array and (D) formation of nanowires by anisotropic Poisson compression.

the protruding NPs to direct aggregation in the unconstrained direction normal to the free edge. Conservation of volume is achieved by expansion in the interchain spacing and polymer and thiol transfer to the underlying polymer film or overlying NP/air interface. Given such a short irradiation time, mass loss of polymer is neglectable.²⁷

Finite element simulations of the bench-scale process (Figure 3A and B) reveal a substantial area of uniform, constrained uniaxial compression, with edge effects (where substantial mixed, shear deformation occurs) confined to the outer perimeter. The simulations were of a quasistatic elastic solid material of the dimensions of the preirradiated film (100 nm × 3 mm × 5 mm). The process of drying and residual stress redistribution was predicted using prestress and mass-loss terms in a Lagrangian framework. The mesh, being Lagrangian in nature, follows the motion of the elastic network, indicating a uniform compression over a large portion of the film (as shown is Figure 3B). Because the Au NPs reside at the polymer surface, we expect their trajectories to be well predicted by the simulation.

To visualize the one-dimensional deformation of the close-packed NP monolayer at the NP scale, we used a molecular dynamics code LAMMPS²⁸ with polymer/solvent/particle interactions incorporated in the Vincent potential, based on Flory–Huggins theory derived for spherical, polymer-coated particles and accounting for (1) bulk-polymer induced depletion, (2) polymer–polymer steric repulsion, and (3) polymer–polymer elastic repulsion. DLVO, polymer, and lubrication forces are all coarse-grained to enable multiscale simulations much larger than DFT or molecular methods can permit. In order to simulate the aspect of sintering, particle diffusivity is artificially restricted and maximum interparticle force is limited during compression such that the particles are forced to overlap slightly. Figure 3C shows a simulated 2D close-packed array of 5.5-nm diameter, alkane-thiolated Au nanoparticles formed from a dilute solution of NPs in toluene/PMMA by solvent removal and equilibration at 298 K. Subjecting the closed packed monolayer to a simulated one-dimensional Poisson

compression with a Poisson ratio of 0.1 (based on the surface aspect ratio of the deformed Lagrangian mesh) and corresponding to that of a nearly incompressible solid results in the formation of chain-like aggregates whose orientation depends on that of the parent close packed array. Comparison of TEM and FFT of both the experimental and simulated systems (Figures 1 and 3) show good agreement (considering the finite size of the simulation), suggesting that the simulation captures the essential physical parameters of self-assembly and one-dimensional deformation into chain-like aggregates.

To understand the further particle coalescence into single-crystal-like nanowires at room temperature, we emphasize that the location of the NPs at the polymer vapor interface reduces mechanical constraints and facilitates depletion of thiol ligands from regions between the approaching particles.^{25,29} This allows nascent particle–particle contact (Figures 1C and 2) and NP reorientation into energetically favored configurations with crystallographically aligned NP–NP interfaces. Ensuing sintering and coarsening driven by the high NP curvature that increases the surface tension of Au and accordingly the associated driving forces^{30–32} continue during room temperature aging (without E-beam irradiation) until a wire-like structure evolves (Figures 1C and 2 inset) that minimizes differential curvature and interfacial energy.

LAMMPS simulations also provide insight into the effect of orientation of the NP monolayer array with respect to the free edge on the ensuing array morphology after uniaxial compression. The original array has 6-fold symmetry; thus the possible compression angles are limited to be in the range from 0° to 30° (0° to –30° are mirror images). Supplementary Figure S5 shows a ‘map’ of hexagonal NP arrays, with original orientations ranging from 0° to +30° with respect to the uniaxial compression direction, at the point of initial particle–particle contact leading to chains, e.g. 0° or 30°, or 2D, quasi-square grids, e.g. 25°. In the 0° orientation, chains form with ~20% compression with only a modest expansion in NP–NP spacing in the direction normal to the compression direction. This simulated result corresponds closely to our experimental results, suggesting that the original NP arrays are preferentially oriented with respect to the free edge. As the free edge forms by interfacial NP assembly at a retracting three-phase liquid/solid/vapor interface,²⁴ we argue that the 0° angle configuration that aligns the NPs normal to the interface is most probable, thereby orienting preferentially the NP array in the transferred film and enabling consistent formation of NP chains and wires. The 0°-oriented contraction is captured by TEM in Figure S3, which shows the interface between NP chains and the parent NP monolayer array and how chains form by one-dimensional contraction in the 0° orientation. Other initial orientations are possible, and edge effects are anticipated near the boundaries of the suspended films (Figure 3B). These could form quasi-square lattices as shown in Figure S2b or wires inclined with respect to the free edge. It is interesting to note that the nanowire arrays have analogies to a quasi-2D thermodynamically defined lamellar mesophase,^{33,34} and defects like dislocations and disclinations are occasionally observed.

The anisotropic wire-like Au nanostructures formed by E-beam irradiation and room temperature aging as in Figure 1C were characterized electronically with a linear four-probe setup over the temperature range 80 to 300 K. For these measurements the inside two probes were separated by about 50–200 μm. The *I*–*V* plot (Figure 4 inset) acquired at room temperature shows linear, Ohmic behavior in the direction parallel to the wire

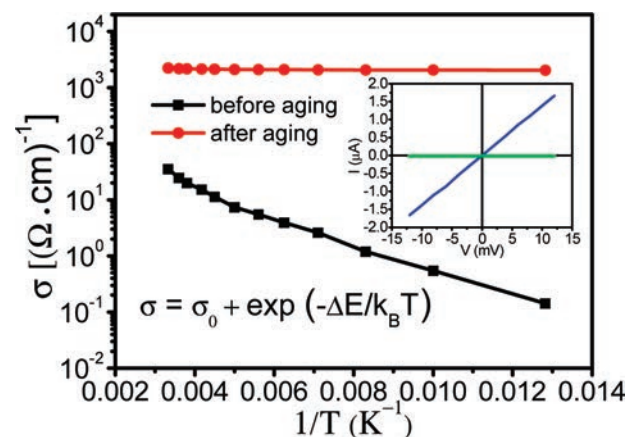


Figure 4. Temperature dependence of conductivity measured for E-beam treated NP film before and after aging process. Inset: *I*–*V* behavior (at 300 K) for irradiated and aged film along the retracting direction (in blue) and in the normal direction (in green).

orientation with the resistivity determined to be 5 kΩ·nm (nearly comparable to that of polycrystalline Au nanowires: 1 kΩ·nm),³⁵ while in the normal direction the array was insulating over the measured range of potential bias (for this probing distance, a much greater voltage needs to be applied to reveal the Coulomb blockade effect⁸). The irradiated sample showed a dramatic change in conductivity before and after the room temperature aging process. The Ohmic *I*–*V* behavior and conductivity of the anisotropic nanostructure after complete sintering and coarsening are independent of temperature, as expected for a metal. However, for the as-irradiated sample without aging, log(σ) was found to vary nearly linearly with $1/T$, corresponding to an effective activation energy of 3.8 meV. This is consistent with that of electrons hopping across the grain boundaries of chain-like aggregates, which behave as a one-dimensional array of quantum islands.

Large scale ordered and oriented metallic nanowire arrays, exhibiting highly anisotropic electrical conductivity, were formed by one-dimensional deformation, reorientation, and sintering of a free-standing close-packed gold NP/polymer monolayer at room temperature. As the individual unit operations, viz. self-assembly, transfer, and e-beam irradiation are all scalable and compatible with traditional semiconductor miniaturized platforms, this approach might be generally applicable for the fabrication and integration of dense, large area, anisotropic nanostructures.

■ ASSOCIATED CONTENT

S Supporting Information. Experimental procedures of monolayer array synthesis and more characterization data are provided. This material is available free of charge via the Internet at <http://pubs.acs.org>.

■ AUTHOR INFORMATION

Corresponding Author
cjbrink@sandia.gov

■ ACKNOWLEDGMENT

This work was supported by the U.S. Department of Energy, Office of Science, Office of Basic Energy Sciences Grant DE-FG02-02-ER15368; the DOE Office of Basic Energy Sciences,

Division of Materials Sciences and Engineering; the National Institute for NanoEngineering (NINE) program at Sandia National Laboratories; and the Sandia National Laboratories' Laboratory Directed Research and Development (LDRD) program. Sandia National Laboratories is a multiprogram laboratory operated by Sandia Corporation, a wholly owned subsidiary of Lockheed Martin Company, for the U.S. Department of Energy's National Nuclear Security Administration under Contract DE-AC04-94AL85000.

REFERENCES

- (1) Brust, M.; Walker, M.; Bethell, D.; Schiffrin, D. J.; Whyman, R. *J. Chem. Soc., Chem. Commun.* **1994**, 801.
- (2) Murray, C. B.; Norris, D. J.; Bawendi, M. G. *J. Am. Chem. Soc.* **1993**, *115*, 8706.
- (3) Talapin, D. V.; Rogach, A. L.; Kornowski, A.; Haase, M.; Weller, H. *Nano Lett.* **2001**, *1*, 207.
- (4) McDonald, S. A.; Konstantatos, G.; Zhang, S. G.; Cyr, P. W.; Klem, E. J. D.; Levina, L.; Sargent, E. H. *Nat. Mater.* **2005**, *4*, 138.
- (5) Sun, S. H.; Anders, S.; Thomson, T.; Baglin, J. E. E.; Toney, M. F.; Hamann, H. F.; Murray, C. B.; Terris, B. D. *J. Phys. Chem. B* **2003**, *107*, 5419.
- (6) Pileni, M. J. *J. Phys. Chem. B* **2001**, 105.
- (7) Middleton, A. A.; Winggreen, N. S. *Phys. Rev. Lett.* **1993**, 71.
- (8) Fan, H. Y.; Yang, K.; Boye, D. M.; Sigmon, T.; Malloy, K. J.; Xu, H. F.; Lopez, G. P.; Brinker, C. J. *Science* **2004**, *304*, 567.
- (9) Shalkevich, N.; Escher, W.; Burgi, T.; Michel, B.; Si-Ahmed, L.; Poulidakos, D. *Langmuir* **2010**, *26*, 663.
- (10) Kovalenko, M. V.; Scheele, M.; Talapin, D. V. *Science* **2009**, *324*, 1417.
- (11) Smith, P. A.; Nordquist, C. D.; Jackson, T. N.; Mayer, T. S.; Martin, B. R.; Mbindyo, J.; Mallouk, T. E. *Appl. Phys. Lett.* **2000**, *77*, 1399.
- (12) Chen, X. Q.; Saito, T.; Yamada, H.; Matsushige, K. *Appl. Phys. Lett.* **2001**, *78*, 3714.
- (13) Tao, A.; Kim, F.; Hess, C.; Goldberger, J.; He, R. R.; Sun, Y. G.; Xia, Y. N.; Yang, P. D. *Nano Lett* **2003**, *3*, 1229.
- (14) Whang, D.; Jin, S.; Wu, Y.; Lieber, C. M. *Nano Lett* **2003**, *3*, 1255.
- (15) Messer, B.; Song, J. H.; Yang, P. D. *J. Am. Chem. Soc.* **2000**, *122*, 10232.
- (16) Huang, Y.; Duan, X. F.; Wei, Q. Q.; Lieber, C. M. *Science* **2001**, *291*, 630.
- (17) Yu, G. H.; Cao, A. Y.; Lieber, C. M. *Nat. Nanotechnol.* **2007**, *2*, 372.
- (18) Yu, G. H.; Li, X. L.; Lieber, C. M.; Cao, A. Y. *J. Mater. Chem.* **2008**, *18*, 728.
- (19) Pevzner, A.; Engel, Y.; Elnathan, R.; Ducobni, T.; Ben-Ishai, M.; Reddy, K.; Shpaisman, N.; Tsukernik, A.; Oksman, M.; Patolsky, F. *Nano Lett.* **2010**, *10*, 1202.
- (20) Javey, A.; Nam, S.; Friedman, R. S.; Yan, H.; Lieber, C. M. *Nano Lett.* **2007**, *7*, 773.
- (21) Fan, Z. Y.; Ho, J. C.; Jacobson, Z. A.; Razavi, H.; Javey, A. *Proc. Natl. Acad. Sci. U.S.A.* **2008**, *105*, 11066.
- (22) Yerushalmi, R.; Jacobson, Z. A.; Ho, J. C.; Fan, Z.; Javey, A. *Appl. Phys. Lett.* **2007**, 91.
- (23) Fan, Z. Y.; Ho, J. C.; Takahashi, T.; Yerushalmi, R.; Takei, K.; Ford, A. C.; Chueh, Y. L.; Javey, A. *Adv. Mater.* **2009**, *21*, 3730.
- (24) Pang, J. B.; Xiong, S. S.; Jaeckel, F.; Sun, Z. C.; Dunphy, D.; Brinker, C. J. *J. Am. Chem. Soc.* **2008**, *130*, 3284.
- (25) Xiong, S. S.; Miao, X. Y.; Spencer, J.; Khripin, C.; Luk, T. S.; Brinker, C. J. *Small* **2010**, *6*, 2126.
- (26) Croll, S. G. *J. Appl. Polym. Sci.* **1979**, *23*, 847.
- (27) Finch, D. S.; Vesely, D. *Polymer* **1987**, *28*, 675.
- (28) Plimpton, S.; Attaway, S.; Hendrickson, B.; Swegle, J.; Vaughan, C.; Gardner, D. J. *Parallel Distr. Com.* **1998**, *50*, 104.
- (29) Lane, J. M. D.; Grest, G. S. *Phys. Rev. Lett.* **2010**, 104.
- (30) Kang, S. L. *Sintering-Densification, Grain Growth, and Microstructure*; Elsevier: Burlington, MA, 2005.
- (31) Chen, Y.; Palmer, R. E.; Wilcoxon, J. P. *Langmuir* **2006**, *22*, 2851.
- (32) Nanda, K. K.; Maisels, A.; Kruis, F. E. *J. Phys. Chem. C* **2008**, *112*, 4.
- (33) Ruiz, R.; Kang, H. M.; Detcheverry, F. A.; Dobisz, E.; Kercher, D. S.; Albrecht, T. R.; de Pablo, J. J.; Nealey, P. F. *Science* **2008**, *321*, 936.
- (34) Bitá, I.; Yang, J. K. W.; Jung, Y. S.; Ross, C. A.; Thomas, E. L.; Berggren, K. K. *Science* **2008**, *321*, 939.
- (35) Song, J. H.; Wu, Y. Y.; Messer, B.; Kind, H.; Yang, P. D. *J. Am. Chem. Soc.* **2001**, *123*, 10397.